J. Fluid Mech. (1991), *vol.* 232, *pp.* 439–453
Printed in Great Britain

Free-surface effects on the spin-up of fluid in a rotating cylinder

By JAMES O'DONNELL[1] AND P. F. LINDEN[2]

[1] Department of Marine Sciences, The University of Connecticut, Groton, Connecticut, USA

[2] Department of Applied Mathematics and Theoretical Physics, The University of Cambridge, Silver St., Cambridge CB3 9EW, UK

(Received 9 May 1990 and in revised form 18 February 1991)

We present a theory for the decay of the relative motion of a homogenous fluid with a free surface in a rotating cylindrical tank with a flat bottom, induced by an abrupt change in the angular velocity. We then describe a set of laboratory experiments designed to test the predictions of the theory.

At low rates of rotation the dynamics of the adjustment is well understood and measurements have verified the established theoretical results that the motion decays exponentially, with a timescale proportional to the rotation period divided by the square root of the Ekman number, and that the relative vorticity remains independent of radius. At higher rotation rates, however, the curvature and motion of the free surface complicate the dynamics, and have hindered the development of a more general theory.

Both the theoretical predictions and the experiments show that at high rotation rates the decay of the relative vorticity is independent of radius and exponential in time, but with a decay timescale, τ_e, that increases linearly with the rotational Froude number F, i.e. $\tau_e = 1 + \frac{1}{16}F$. An analysis of the vorticity dynamics during spin-up indicates that, near the centre of the tank, this simple behaviour is the result of vigorous competition between the rate of vortex line stretching by Ekman-layer pumping and surface deformation. Near the boundary, these mechanisms cooperate, but are partially offset by the stretching produced by the secondary radial circulation.

1. Introduction

The search for a theoretical description of the fluid motion in a rotating cylinder caused by an abrupt change in the rotation rate has stimulated a considerable amount of research. The problem is of fundamental interest to geophysical fluid dynamicists because it is a simple and controllable analogue of some of the features of the large-scale circulation of the ocean and atmosphere (Holton 1965). It also has direct application to the behaviour of liquid fuel in spin-stabilized projectiles and satellites (Goller & Ranov 1968).

Three parameters determine the mechanism and rate of spin-up in fluids of uniform density: the Rossby number, $\epsilon = \Delta\Omega/\Omega$, the ratio of the change in angular velocity of the tank to the final angular velocity; the Froude number, $F = 4\Omega^2R^2/gH$, where R is the radius of the cylinder, H is the depth of the fluid and g is the acceleration due to gravity; and the Ekman number, $E = \nu/\Omega H^2$, where ν is the kinematic viscosity of the liquid. Greenspan & Howard (1963) and Greenspan (1964, 1965) made a comprehensive theoretical study of the spin-up of a homogeneous fluid

completely filling a closed cylinder for small ϵ and E and obtained results that have shown good agreement with experiments. These studies are summarized by Greenspan (1968) and it is now well known that the secondary radial circulation induced by the frictional boundary layers at rigid surfaces, the 'Ekman layers', causes the azimuthal velocity scaled by $\Delta\Omega$, denoted here by u_θ, to decay exponentially with a decay timescale $\tau = 1/\Omega E^{\frac{1}{2}}$. Outside these boundary layers

$$u_\theta = \epsilon r \exp(-t/\tau), \tag{1}$$

where r is the radial coordinate scaled by the radius of the container.

This result must be modified when the upper boundary of the fluid is a (parabolic) free surface since then vortex lines may be 'stretched' or 'squashed' as they move radially. Greenspan & Howard (1963, hereinafter referred to as GH63) developed a more general theory for small F which, in the special case of a fluid contained in a right circular cylinder with a flat bottom, predicts that the azimuthal velocity evolves as,

$$u_\theta(r,t) = \epsilon r\left[1+\frac{F}{16}\frac{t}{\tau}\right]\exp\left(\frac{-t}{\tau}\right). \tag{2}$$

The additional factor in (2) shows that the effect of the free surface is to delay spin-up by an amount proportional to F, and that the radial dependence of u_θ remains linear so the liquid spins up as a solid body. Measurements of velocity in an experiment with $F = 0.75$ showed close agreement with this theoretical prediction.

More recently, Cederlof (1988) has further investigated the role of the free surface in the spin-up problem. He developed a theory for the decay of the relative motion of homogeneous fluid in a cylindrical container with a parabolic bottom shape chosen to be identical to the surface parabola. The advantage of this geometry is that it retains the influence of the vertical movement of the free surface, but eliminates the mechanism of vortex stretching by the radial secondary flow and the associated mathematical difficulty that restricted the GH63 result to small F. Both Cederlof's model and laboratory experiments demonstrated that only the outer region of the cylinder, of order $RF^{-\frac{1}{2}}$ from the wall, spins up with a timescale τ, while the interior of the fluid spins up in the much longer timescale $F\tau$. This delay in the spin-up was attributed to the motion of the free surface.

In the next section of this paper we present a quasi-geostrophic theory for the spin-up of the motion of a fluid with a free surface in a flat-bottomed, cylindrical tank. In §3 we describe a set of experiments to test the predictions of the theory and present the results in §4. In the concluding section we discuss the vorticity dynamics of the spin-up process and summarize the conclusions of this work.

2. Theory

The horizontal momentum equations in a frame of reference rotating at Ω, for a hydrostatic, axisymmetric flow with small Ekman number, E, are

$$\frac{\partial u_r}{\partial t}+u_r\frac{\partial u_r}{\partial r}+w\frac{\partial u_r}{\partial z}-\frac{u_\theta^2}{r}-2\Omega u_\theta = -g\frac{\partial}{\partial r}(\eta+N)+\Omega^2 r, \tag{3}$$

and

$$\frac{\partial u_\theta}{\partial t}+u_r\frac{\partial u_\theta}{\partial r}+w\frac{\partial u_\theta}{\partial z}+\frac{u_\theta u_r}{r}+2\Omega u_r = 0, \tag{4}$$

where $N(r)$ is the surface deformation in the absence of relative motion and $\eta(r,t)$ is that due solely to the motion. It is well established that when $E \ll 1$ the only influence

of bottom friction on the interior motion is to force a vertical velocity at the top of the bottom Ekman layer; see, for example, Greenspan (1968). After integration in z from the bottom, $z = -h(r)$, to the surface, $z = \eta(r,t)+N(r)$, the continuity equation for an incompressible fluid is

$$\frac{1}{r}\frac{\partial}{\partial r}\{ru_r[N(r)+h(r)+\eta(r,t)]\}+\frac{\partial\eta}{\partial t}-\frac{\delta_E}{2r}\frac{\partial ru_\theta}{\partial r}=0, \tag{5}$$

where $\delta_E = (\nu/\Omega)^{\frac{1}{2}}$, the bottom Ekman-layer thickness, sets the magnitude of the vertical velocity at the bottom.

These equations may be made dimensionless by defining the new variables:

$$\tilde{r}=\frac{r}{R};\quad \tilde{z}=\frac{z}{H};\quad \tilde{t}=\frac{t}{E^{-\frac{1}{2}}\Omega^{-1}};\quad \tilde{u}_\theta=\frac{u_\theta}{\epsilon\Omega R};\quad \tilde{u}_r=\frac{u_r}{\epsilon\Omega RE^{\frac{1}{2}}};$$

$$\tilde{w}=\frac{w}{\epsilon\Omega HE^{\frac{1}{2}}};\quad \tilde{\eta}=\frac{\eta}{2\Omega^2R^2g^{-1}\epsilon};\quad \tilde{N}=\frac{N}{2\Omega^2R^2g^{-1}};\quad \tilde{h}=\frac{h}{H},$$

so that substitution in (3), (4) and (5) gives

$$\epsilon\left[E\left\{\frac{\partial u_r}{\partial t}+\epsilon\left(u_r\frac{\partial u_r}{\partial r}+w\frac{\partial u_r}{\partial z}\right)\right\}-\epsilon\frac{u_\theta^2}{r}-2u_\theta\right]=-2\frac{\partial}{\partial r}\{\epsilon\eta+N\}+r, \tag{6}$$

$$\frac{\partial u_\theta}{\partial t}+\epsilon\left\{u_r\frac{\partial u_\theta}{\partial r}+w\frac{\partial u_\theta}{\partial z}+\frac{u_\theta u_r}{r}\right\}+2u_r=0, \tag{7}$$

and

$$\frac{1}{r}\frac{\partial}{\partial r}[ru_r(\tfrac{1}{2}FN+\tfrac{1}{2}\epsilon F\eta+h)]+\tfrac{1}{2}F\frac{\partial\eta}{\partial t}-\frac{1}{2}\frac{1}{r}\frac{\partial ru_\theta}{\partial r}=0, \tag{8}$$

where $F = 4\Omega^2R^2/gH$ and the variables have been written without the tildes for clarity of presentation. Note, however, that all variables are henceforth dimensionless. It has been demonstrated by Greenspan (1968) that the appropriate boundary condition at $r = 1$ requires that the interior radial flux balances that in the Ekman layer, thus

$$\{\tfrac{1}{2}FN(1)+\tfrac{1}{2}\epsilon F\eta(1,t)+h(1)\}u_r(1,t)-\tfrac{1}{2}u_\theta(1,t)=0. \tag{9}$$

In the absence of relative motion, (6) and the volume conservation constraint $\int_0^1 rN(r)\,dr = 0$ implies that the free surface is parabolic with

$$N(r)=\tfrac{1}{4}(r^2-\tfrac{1}{2}). \tag{10}$$

The dimensional thickness of the fluid layer at the centre of a flat-bottomed tank is then $H(1-\frac{1}{16}F)$, and zero for $F \geqslant 16$. In this paper we consider only cases where the layer depth is non-zero everywhere, i.e. $0 \leqslant F \leqslant 16$, and seek solutions for $1 \gg \epsilon F > \epsilon$ by expanding the variables in power series as

$$\begin{aligned}\eta &= \eta_0+\epsilon\eta_1+\epsilon^2\eta_2+\dots,\\ u_\theta &= u_{\theta0}+\epsilon u_{\theta1}+\epsilon^2u_{\theta2}+\dots,\\ u_r &= u_{r0}+\epsilon u_{r1}+\epsilon^2u_{r2}+\dots.\end{aligned} \tag{11}$$

To lowest order in ϵ, (6) and (7) yield the familiar geostrophic balance relations

$$u_{\theta0}=\frac{\partial\eta_0}{\partial r} \tag{12}$$

and
$$\frac{\partial u_{\theta 0}}{\partial t} = -2u_{r0}. \tag{13}$$

The corresponding integrated continuity equation, (8), is then

$$\frac{1}{r}\frac{\partial}{\partial r}[ru_{r0}(\tfrac{1}{2}FN+h)]+\tfrac{1}{2}F\frac{\partial \eta_0}{\partial t}-\frac{1}{2r}\frac{\partial r u_{\theta 0}}{\partial r} = 0, \tag{14}$$

and the boundary condition at $r = 1$ is

$$(\tfrac{1}{2}FN+h)\,u_{r0}|_{r=1} = \tfrac{1}{2}u_{\theta 0}|_{r=1} \tag{15}$$

Substitution of (12) and (13) in (14) enables the elimination of the velocities in favour of the surface deformation and the problem may then be concisely restated as

$$F\frac{\partial \eta_0}{\partial t}-\frac{1}{r}\frac{\partial}{\partial r}r\left(\frac{\partial \eta_0}{\partial r}+(\tfrac{1}{2}FN+h)\frac{\partial^2 \eta_0}{\partial t\,\partial r}\right) = 0, \tag{16}$$

with the boundary condition

$$(\tfrac{1}{2}FN+h)\frac{\partial}{\partial t}\frac{\partial \eta_0}{\partial r}\bigg|_{r=1} = -\frac{\partial \eta_0}{\partial r}\bigg|_{r=1}. \tag{17}$$

Note, if we now select $h(r)$ such that $h+\frac{1}{2}FN = 1$ then (16) and (17) are identical to equations (2.12) and (2.14) of Cederlof (1988). The two unnumbered equations following (2.14) in Cederlof's paper have a slight error however, and should be the same as (16) and (17).

Substitution of (10) and $h = 1$ in (17), followed by an integration, yields the boundary condition

$$\frac{\partial \eta_0}{\partial r}\bigg|_{r=1} = u_{\theta 0}\bigg|_{r=1} = \exp\left\{\frac{-t}{1+\frac{1}{16}F}\right\}. \tag{18}$$

If we now require that the initial surface deformation be in geostrophic balance with a velocity $u_{\theta 0}(r, t = 0) = r$, the initial condition applicable to the spin-up problem, then

$$\eta_0(r, t = 0) = \tfrac{1}{2}(r^2-\tfrac{1}{2}). \tag{19}$$

This problem may then be solved for smooth-bottom geometries by the method of integral transforms or numerical techniques, but for $h(r) = 1$ it is easily verified that

$$\eta_0(r, t) = \tfrac{1}{2}(r^2-\tfrac{1}{2})\exp\left\{\frac{-t}{1+\frac{1}{16}F}\right\} \tag{20}$$

satisfies (16), (18) and (19), and is therefore a valid solution. The corresponding azimuthal velocity field evolves as

$$u_{\theta 0}(r, t) = r\exp\left\{\frac{-t}{1+\frac{1}{16}F}\right\} \tag{21}$$

which, as can be demonstrated by a Taylor series expansion for small F, is a generalization of (2), the GH63 result. The theory predicts then that the fluid motion will spin-up as a solid body, as did earlier work, but with a decay timescale that increases with F.

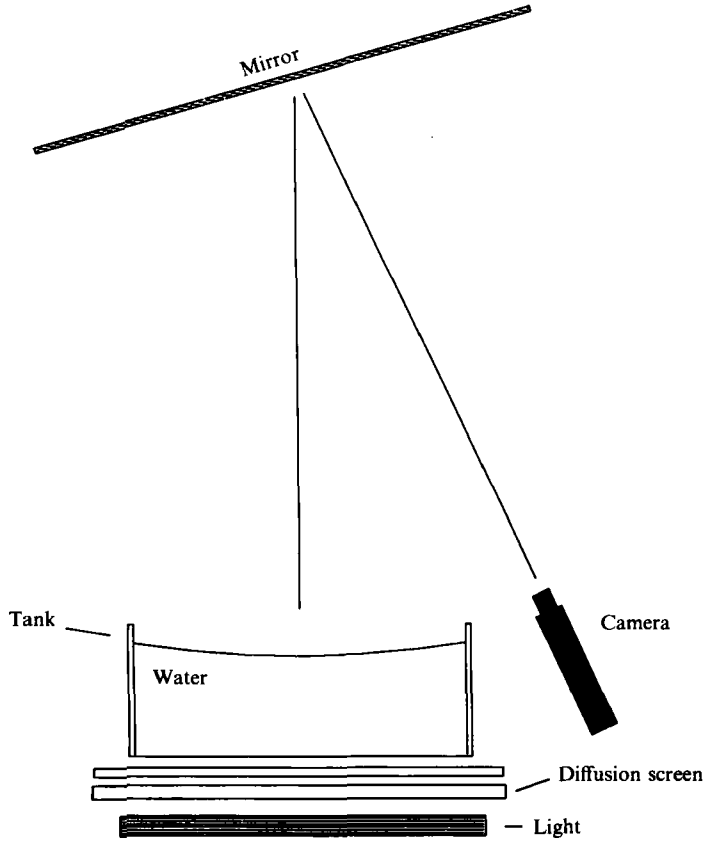

FIGURE 1. A schematic of experimental equipment.

3. Experiments

To test the predictions of this theory, we performed 11 experiments on a highly stable and precisely controlled rotating table. With the apparatus sketched in figure 1 assembled on the table, measurements of the rotation rate showed variations of less than 0.001 rad/s about the selected value. Experiments were conducted with distilled water contained in a 0.5 ± 0.001 m steel cylinder with a glass bottom and a removable glass lid. The tank was supported over a diffuse fluorescent light source by an anodized aluminium frame and an image of the fluid motion was recorded by a high-resolution, solid-state video camera connected to a video cassette recorder through slip rings. The tank was filled to the required depth, and the table was set to the selected rotation rate Ω. After the initial relative motion had decayed, the lid was temporarily removed while between 20 and 40 small circular pieces of black paper were scattered randomly on the surface of the water visualize the motion. This procedure generally resulted in some wave motion which decayed quite quickly. Subsequently, the experiments was initiated by abruptly changing the rotation rate to $\Omega + \Delta\Omega$. Parameter values and measured variables for all the experiments discussed are presented in table 1.

Velocity estimates were obtained by measuring the displacement of particles over a known time interval. This simple procedure was automated by playing the recording of the experiments to a video digitizer and microcomputer which located and stored the positions of the centre of each particle in a chosen frame. The net

Experiment	F	Ω (rad/s)	ϵ	depth (mm)	$E^{\frac{1}{2}}$ $\times 10^3$	τ_e
1	0.379	1.000	0.167	97	9.41	1.09
2	0.545	1.200	0.167	97	8.59	1.01
3	1.515	2.000	0.167	97	6.65	1.16
4	2.181	2.440	0.153	97	6.07	1.23
5	2.657	2.300	0.080	60	10.5	1.17
6	6.199	3.000	−0.111	30	20.3	1.36
7	11.480	2.700	0.100	20	28.9	1.80
8	15.306	2.700	0.100	15	38.5	1.97
9	0.095	0.500	0.167	97	13.3	1.15
10	4.500	2.700	0.091	50	11.6	1.27
11	8.62	2.400	0.077	20	31.0	1.58

TABLE 1: A summary of the experiments

angular and radial movement of each particle between successive frames was then calculated. Since the radial component of velocity during spin-up is much smaller, $O(E)$, than the azimuthal component, and since the uncertainty associated with these estimates is limited by the ratio of the net displacement to the radius of the particles, particle positions at two times separated by $O(\Omega^{-1})$ enables the estimation of only u_θ with acceptable uncertainty. Near the centre of the tank however, particle displacements are always small and uncertainties large. Therefore, measurements in the interval $0 \leqslant r \leqslant 0.1$ were ignored.

In the following discussion of the analysis of results, the evolution of the angular velocity of the fluid, $\omega = u_\theta / r\Delta\Omega$, is employed since it is expected to be independent of r and is more convenient to display.

When a velocity decay is exponential, the use of $(\theta(t_2)-\theta(t_1))/(t_2-t_1)$ as an estimate of the angular velocity introduces a systematic error; the velocity is always overestimated. This is a only minor problem when the t_2-t_1 is small compared to decay timescale but, when the velocity is small, a longer time is required to achieve a suitably large $\theta(t_2)-\theta(t_1)$, and the error can be important. A simple correction is possible, however, which exploits information about the decay rate obtained from all the velocity measurements in an experiment and thus was applied to all observations. The derivation is outlined, and a brief discussion of the consequences of the correction are presented in the Appendix.

4. Results

In figure 2 we present the evolution of the angular velocity, observed in experiment 1, in which $F = 0.38$, to demonstrate that the experimental method reliably replicates the well-established theory of GH63 for small F. The data values shown are the average of at least five measurements of the angular velocity in the interval $r = 0.1$–0.9 and are plotted with error bars showing the standard deviation of the measurements. Additionally, the theoretical behaviour for spin-up in a closed cylinder, equation (1), is indicated by the dashes and the GH63 correction for small F, equation (2), is shown by the solid line and is in good agreement with the data at this low value of F.

In figure 3 the radial distributions of the angular velocity obtained in three experiments with $F = 2.657, 6.199$ and 15.306 are shown. The error bars indicate the

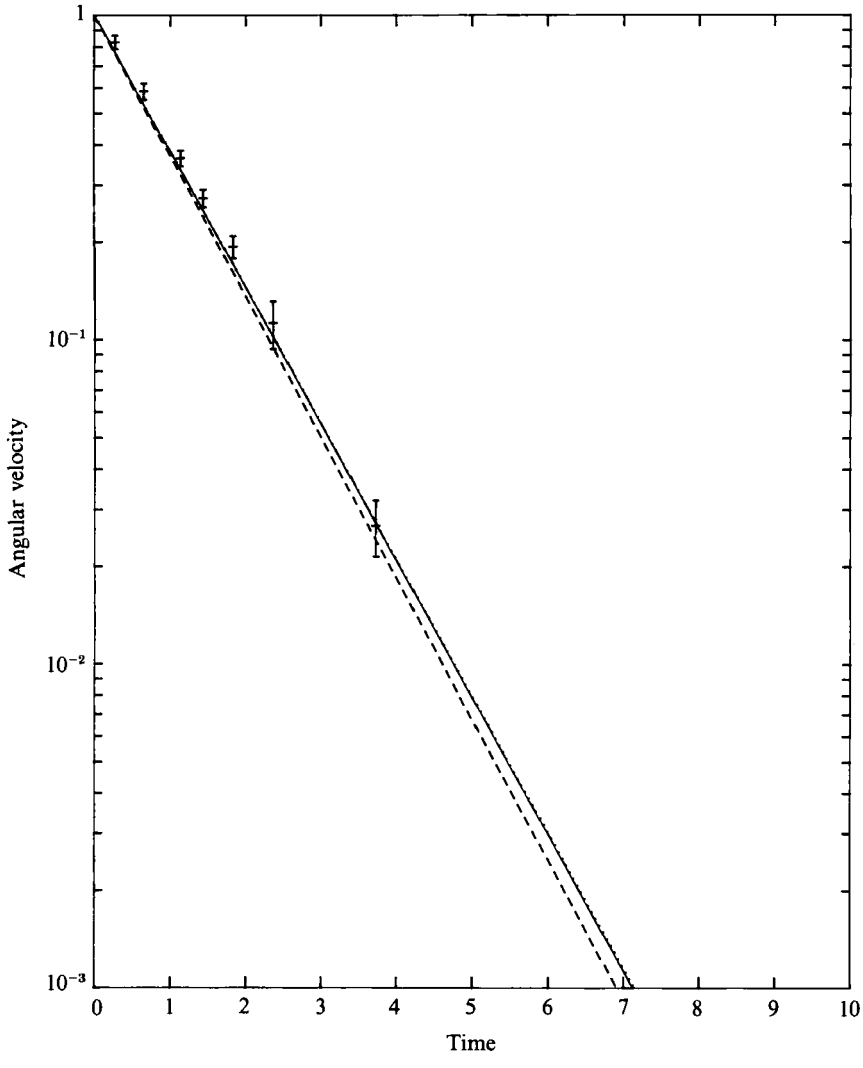

FIGURE 2. A plot of the observed angular velocity evolution in experiment 1 in which $F = 0.379$. Variables are dimensionless and each point represents the radial average of data in the interval $0.1 \leqslant r \leqslant 0.9$ and the error bars indicate the standard deviation of the mean. The dashed line shows $\exp(-t)$ and the solid line, the Greenspan & Howard (1963) theory for small F. Linear regression through the data yields the line indicated by the dots.

uncertainty in the velocity estimates, due primarily to uncertainty in the measurements in particle positions, and the horizontal lines show the velocities predicted using (21) at the times indicated on the right of the figures. The data are consistent with the theoretical prediction that the angular velocity is uniform and are also close to the predicted magnitude. There appears to be more scatter in the data than can be explained by the uncertainty associated with the measurements but since most of the scatter occurs early in the experiment when observing intervals were short, the large variance may be the result of the aliasing of near inertial frequency motions, although an intrinsic flow instability cannot be ruled out.

The consistency of the observed and predicted temporal behaviour is evident in figure 4, which displays the evolution of the angular velocity, averaged radially from

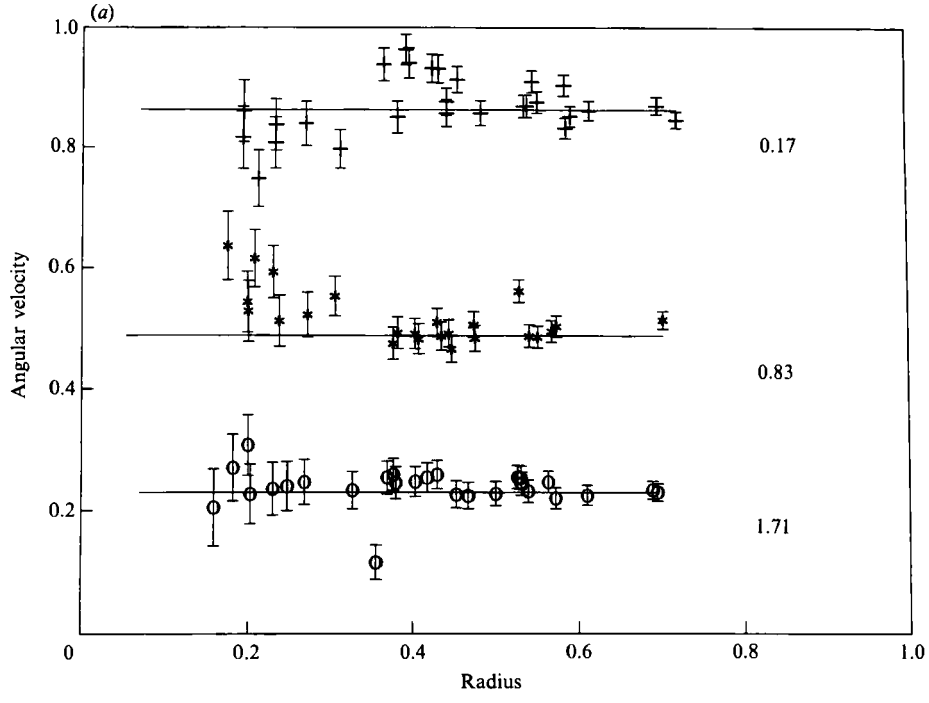

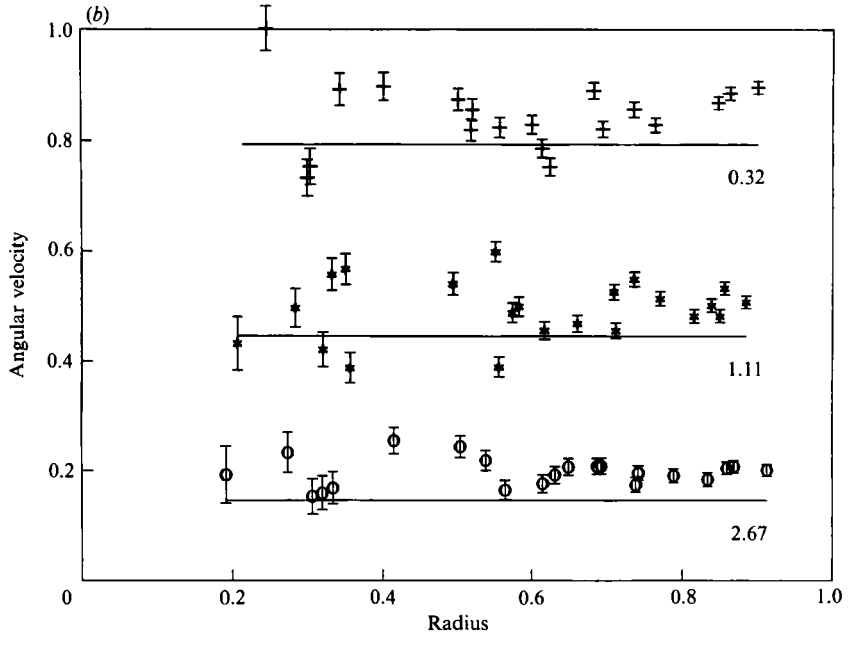

FIGURE 3(*a*, *b*). For caption see facing page.

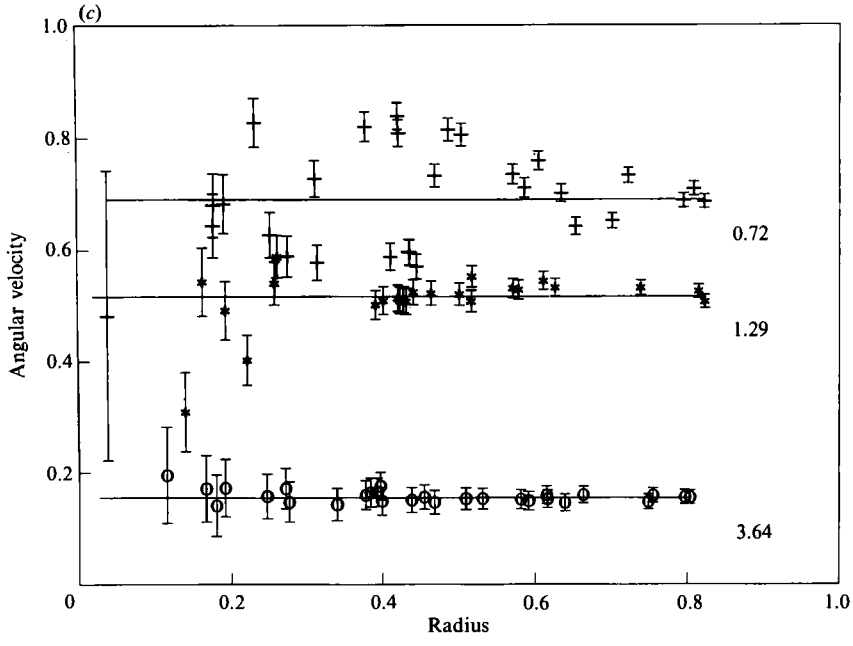

FIGURE 3. Plots of the radial distribution of the angular velocities observed in (*a*) experiment 5, (*b*) 6, and (*c*) 8, in which $F = 2.657$, 6.199, and 15.306, respectively. Observations and theoretical predictions are shown at three dimensionless times for each experiment. The crosses are associated with the smallest time, the asterisks with the intermediate time, and the circles with the largest time. Error bars indicate the estimated uncertainty in the measurements. The horizontal lines are the predictions of (21).

$r = 0.1$ to 0.9, in experiments with $F = 2.657$, 11.480 and 15.306. Here the error bars indicate the standard deviation of the mean and, as in figure 2, the behaviour predicted by equations (1) and (2) is indicated by the dashed and the solid lines. The predictions of the theory presented in §2 (equation (21)) are shown by the dotted lines. It is clear in figure 4(*a*) that the spin-up rate differs significantly from the simple theory, (1), at $F = 2.657$ and that the GH63 theory, (2), satisfactorily describes the observations. Figures 4(*b*) and 4(*c*) show that spin-up is delayed at higher Froude numbers and that the simple theories appear to be inadequate. The data show good agreement with the predictions of the new theory, supporting its validity.

The results of the experiments can be summarized by a comparison of the predicted and observed dependence of spin-up rates on the Froude number as is displayed in figure 5. The decay scales in each experiment were obtained by regression of the radially averaged angular velocity data with elapsed time. The lower line in the figure shows $1 + \frac{1}{16}F$, the theoretical spin-up time, and the upper line shows the best fit to the observed spin-up times. Though there is a slight offset, the lines are almost parallel and indicate that the theory is a good description of the dynamics. The observed decay timescale at $F = 6.199$ (experiment 6) in the one experiment with spindown is anomalously high however, and we are currently investigating the nonlinear generalization of the theory to seek an explanation of this result.

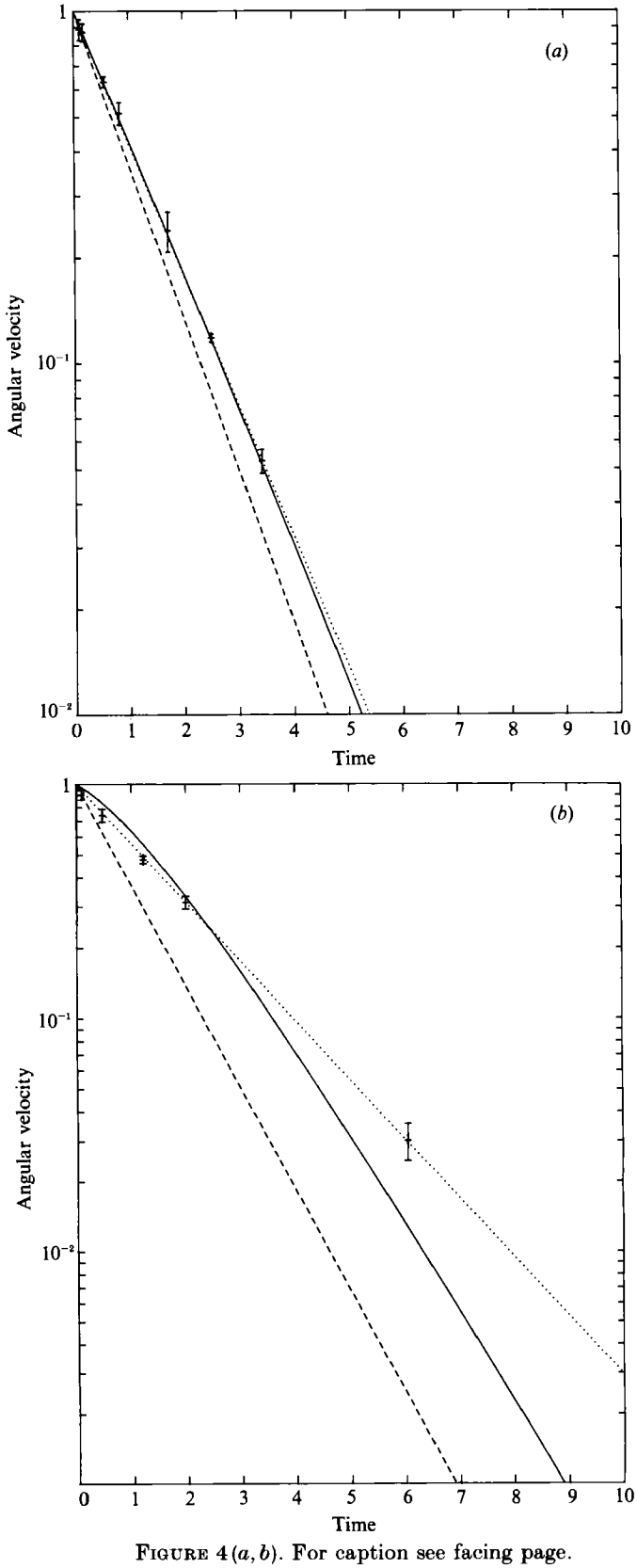

FIGURE 4 (*a*, *b*). For caption see facing page.

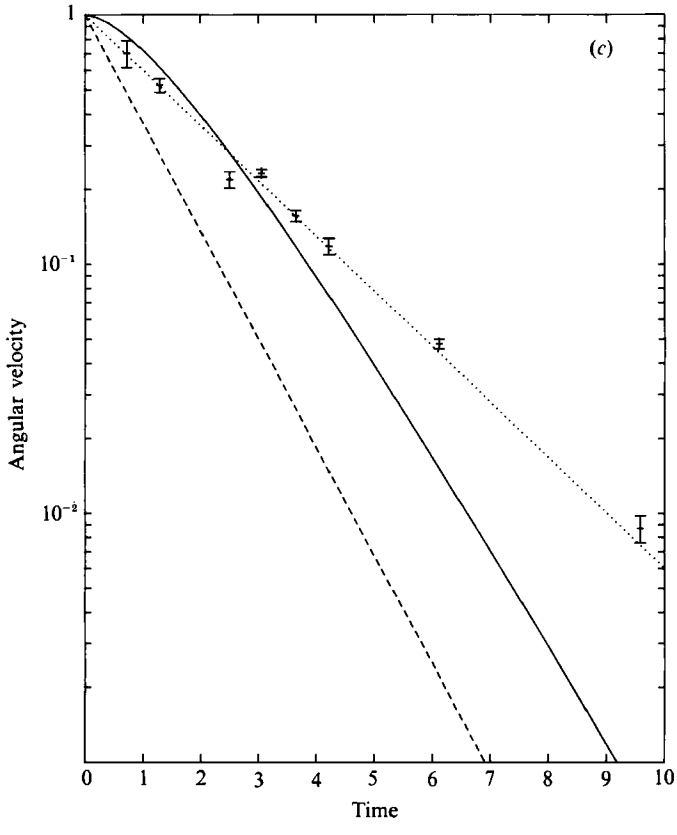

FIGURE 4. Plots of the observed angular velocity evolution for (*a*) experiment 5 (*b*) 6, and (*c*) 8, in which $F = 2.657$, 11.480, and 15.306, respectively. Each point represents the radial average of data in the interval $0.1 \leqslant r \leqslant 0.9$ and the error bars indicate the standard deviation of the mean. The dashed line indicates exp $(-t)$ and the solid line, the Greenspan & Howard (1963) theory for small F. The dotted line shows the prediction of the present theory.

5. Discussion and conclusions

Why is there such simple behaviour? Although the presence of the free surface introduces several new mechanisms to the vorticity dynamics of spin-up, the simple results of Greenspan & Howard (1963), that the vorticity remains spatially uniform as it decays exponentially, remain valid at high Froude numbers.

Cederlof (1988) demonstrated that, for small F, the effects of mechanisms that introduce non-uniformities cancel at lowest order but when the influence of the surface curvature is eliminated by choosing a parallel bottom, significant radial structure develops with rapid spin-up in the outer region and delayed spin-up in the interior. We must conclude therefore that it is the vertical motion of the surface that is responsible for the delay of spin-up and, in a flat-bottomed tank, the geometric effects combine to inhibit spin-up near the tank walls and to enhance spin-up in the centre of the tank. We now briefly examine this rather delicate and interesting competition.

The influences of the free surface are most clear in the potential vorticity form of equation (16) which, for the special case of a flat-bottomed cylinder ($h = 1$), is

$$\{1+FN(r)\}\frac{\partial \xi_0}{\partial t} = -\xi_0 + F\frac{\partial \eta_0}{\partial t} + Fu_{r0}\frac{\partial N(r)}{\partial r}, \tag{22}$$

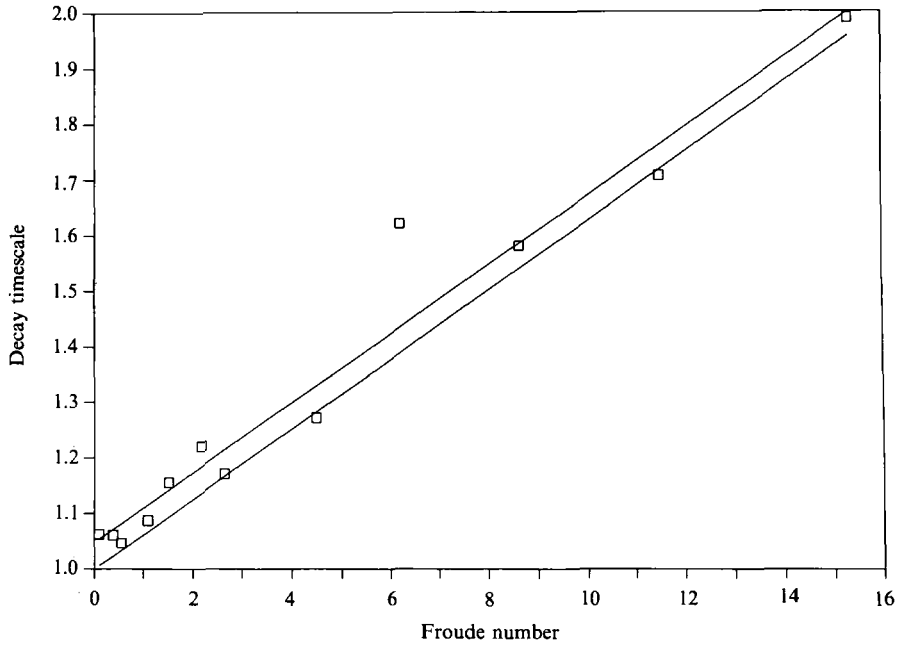

FIGURE 5. Plot of the decay constant τ_e obtained by regression for all experiments, as a function of Froude number. The upper line indicates the best fit to the data and the lower line the theoretical behaviour.

where $$\xi_0 = \frac{1}{r}\frac{\partial}{\partial r}\left(r\frac{\partial \eta_0}{\partial r}\right)$$

is the relative vorticity. The term on the left-hand side of (22) is the rate of change of the quasi-geostrophic potential vorticity which, for small Rossby numbers, ϵ, is determined by rate of the stretching of planetary vortex lines by Ekman-layer pumping and the motion of the free surface (the first and second terms on the right-hand side) and by vortex line stretching by the motion in the direction of the background potential vorticity gradient.

The free surface in a rotating tank of fluid at high rotation rates modifies spin-up by (i) causing the bottom Ekman-layer pumping to be spatially variable, (ii) allowing stretching by the free-surface motion, (iii) introducing stretching by the radial circulation, and (iv) controlling the magnitude of the interior radial velocity through the outer boundary condition, equation (15). Note, however, that as Cederlof (1988) has pointed out, only $F\,\partial\eta_0/\partial t$ is a *free* surface effect since the others would be unchanged if a frictionless, rigid parabolic lid enclosed the fluid.

Since a solution has been obtained in which ξ is uniform even though the vorticity modification processes represented on the right of (22) are functions of radius, the relative importance of each of the mechanisms must be independent of time and sum to a constant at all r. This can be demonstrated by a simple manipulation of (22), using (20) to yield

$$\frac{\partial \xi_0}{\partial t} = -\frac{\xi_0}{1+\frac{1}{16}F}\left\{\frac{1+\frac{1}{16}F}{1+\frac{1}{8}F(r^2-\frac{1}{2})} + \frac{F(r^2-\frac{1}{2})}{4(1+\frac{1}{8}F(r^2-\frac{1}{2}))} - \frac{Fr^2}{8(1+\frac{1}{8}F(r^2-\frac{1}{2}))}\right\}, \tag{23}$$

where the terms in the curly brackets, i.e. the vortex stretching by Ekman-layer pumping, surface deformation and the radial circulation, sum to unity.

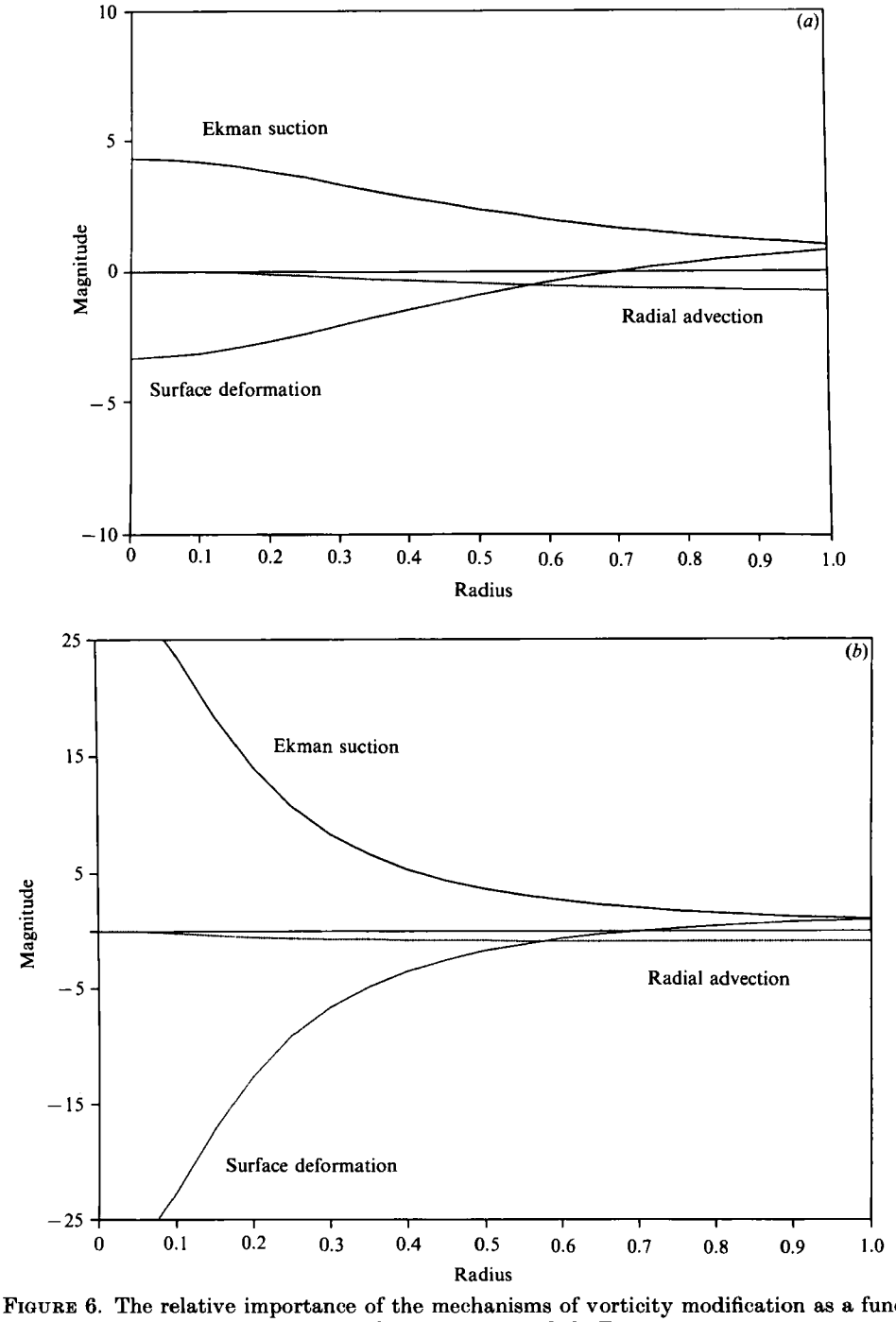

FIGURE 6. The relative importance of the mechanisms of vorticity modification as a function of radius for (*a*) $F = 10$ and (*b*) $F = 15$.

We can conclude immediately from (23) that, since the first and third terms on the right are of opposite sign, vortex stretching by the secondary radial circulation must always compete with the Ekman pumping to delay spin-up, and that, since the second term changes sign at $r = 2^{-\frac{1}{2}}$, vortex stretching by the motion of the surface

cooperates with the Ekman pumping in the outer region of the tank, but hinders spin-up in the centre. Figure 6 displays this behaviour quantitatively, showing the magnitude of each of the three terms in the bracket on the right-hand side of (23) as a function of r for $F = 10$ figure (6*a*) and 15 (figure 6*b*). In both cases it is clear that it is the geometric effect of vortex stretching by the radial motion that counteracts the tendency of the surface motion to enhance spin-up in the outer part of the tank. Indeed, at the outer boundary, advective stretching exactly offsets that caused by the surface motion. In the centre of the tank, vortex stretching by the Ekman-layer pumping is enhanced by the shallowness of the layer but this is offset to a large extent by the movement of the surface. As F approaches 16, the equilibrium thickness of the layer at the centre of the tank tends to zero and the rate of change of vorticity during spin-up is the result of the small imbalance between two large competing processes.

In summary, we have presented a theory that explains the observed spin-up of a homogeneous fluid with a free surface contained in a rotating cylinder with a flat bottom for the full range of Froude numbers up to the value at which the free surface touches the bottom at the centre of the tank. Comparison of the predictions of the theory to the results of experiments in which we observed the evolution of the angular velocity show excellent agreement. Both the theory and observations agree that the angular velocity of the free-surface flow spins-up uniformly but more slowly than that in a closed cylinder. The timescale of the exponential decay increases with the rotational Froude number F as $1+\frac{1}{16}F$.

This work was supported by the Natural Environmental Research Council of Great Britain and the United States National Science Foundation (OCE-8816566). It would have been impossible but for the expertise of the DAMTP laboratory technicians. We are also grateful to Drs Stuart Dalziel, Hiroshi Niino, and David Smeed for their insight and help in the lab, to Dr Tony Howes for helpful suggestions on numerical methods, and to Richard Perkins and Julian Hayward who provided assistance in the digital image analysis.

Appendix

Since the angular velocity ω is a decaying exponential function of t/A, the estimate of angular velocity $\hat{\omega} = (\theta_2-\theta_1)/(t_2-t_1)$, where $\theta_i = \theta(t = t_i)$ is the angular position of a particle, contains a systematic error of order $((t_2-t_1)/A)^2$. This is made evident, and the correction can be derived, by considering

$$\theta_2-\theta_1 = \int_{t=t_1}^{t_2} \omega(t)\,\mathrm{d}t, \tag{A 1}$$

and since $\omega(t) = \mathrm{e}^{-t/A}$, where A is a constant,

$$\theta_2-\theta_1 = A\,(\mathrm{e}^{-t_1/A}-\mathrm{e}^{-t_2/A}). \tag{A 2}$$

A simple Taylor series expansion of the exponential functions yields the order of the error. Assume for the moment that we know A; we may then seek the value t_c for which $\hat{\omega}$ most closely approximates $\omega(t_c)$, i.e.

$$t_c = -A \ln\left\{\frac{A}{t_2-t_1}(\mathrm{e}^{-t_1/A}-\mathrm{e}^{-t_2/A})\right\}. \tag{A 3}$$

This formula then enables the correction of the time of the estimate rather than the value of the angular velocity.

The value of A must be determined from data however, and in the analysis of the experiments discussed in this paper, we used the fact that A is close to 1 and employed (A 3) to make initial correction to all the measurements and then made a second correction using a value of A obtained by regression. A second regression was then performed to obtain the values of τ_e reported in table 1. In most experiments the difference between the values of τ_e obtained with and without the correction were of order 0.02. In experiments 6, 8, and 11 the differences were of order 0.1.

REFERENCES

CEDERLOF, U. 1988 Free-surface effects on spin-up. *J. Fluid Mech.* **187**, 395–407.

GOLLER, H. & RANOV, T. 1968 Unsteady rotating flow in a cylinder with a free surface. *Trans. ASME* D: *J. Basic Engng* **90**, 445–454.

GREENSPAN, H. P. 1964 On the transient motion of a contained rotating fluid. *J. Fluid Mech.* **21**, 673–696.

GREENSPAN, H. P. 1965 On the general theory of contained rotating fluid motions. *J. Fluid Mech.* **22**, 449–462.

GREENSPAN, H. P. 1968 *The Theory of Rotating Fluids.* Cambridge University Press.

GREENSPAN, H. P. & HOWARD, L. N. 1963 On the time-dependent motion of a rotating fluid. *J. Fluid Mech.* **17**, 385–404 (referred to herein as GH63).

HOLTON, J. R. 1965 The influence of viscous boundary layers on transient motions in a stratified rotating fluid: part 1. *J. Atmos. Sci.* **22**, 402–411.